

Photoproduction of Positive Pions in Hydrogen-Magnetic Spectrometer Method*

R. L. WALKER, J. G. TEASDALE, V. Z. PETERSON, AND J. I. VETTE
California Institute of Technology, Pasadena, California

(Received March 7, 1955)

Positive pions produced in a cold, high-pressure hydrogen gas target by the 500-Mev bremsstrahlung of the CalTech synchrotron, have been analyzed by a large magnetic spectrometer. The photoproduction cross section has been measured as a function of photon energy at laboratory angles of 12.5° , 30° , 51° , 73° , 104° , 140° , and 180° . The energy region covered depends somewhat on the angle, but is typically from 200 to 470 Mev. From these excitation curves the angular distribution of the photopions in the center of momentum system is obtained for various photon energies, and these angular distributions are analyzed in the form $A + B \cos\theta + C \cos^2\theta$. The angular distribution has a backward maximum at low energies and a forward maximum at high energies, the coefficient B changing sign at about 340 Mev. The total cross section shows a striking maximum near 290 Mev, of magnitude 205×10^{-30} cm², and falls off above the maximum faster than λ^2 .

INTRODUCTION

THE nature of the interaction between pions and nucleons may be investigated most directly, perhaps, by measurements of the scattering of pions by nucleons. Many such pion-nucleon scattering experiments have been performed, and the results analyzed in terms of scattering phase shifts.^{1,2} The analysis does not yield unique results, and the problem of deciding which phase shifts are probably the correct ones has been extensively investigated by de Hoffmann, Metropolis, Alei, and Bethe.²⁻⁴

A closely related process is photopion production, which involves the interaction between photons and the two particles, pion and nucleon, as well as the interaction between pion and nucleon themselves.

The first measurements of the photoproduction of positive pions in hydrogen were those of Steinberger and Bishop⁵ at Berkeley. They measured the cross section at 90° in the laboratory between photon energies 170 and 320 Mev, using targets of polyethylene and carbon, and making a subtraction to obtain the cross section in hydrogen. The pions were identified by requiring a delayed coincidence from the $\pi-\mu-e$ decay. The pion energy was obtained from its range in aluminum absorber placed between target and counter. Steinberger and Bishop found that the excitation curve at 90° seemed to reach a maximum near 290 Mev and was either flat or starting to decrease between 280 and 310 Mev. They also measured the angular distribution at 255 Mev between 60° and 160° in the center of mass system, and found a maximum in the backward

hemisphere. These results have been verified in succeeding work.

Further measurements of photopion production in hydrogen have been made at Berkeley by White, Jacobson, and Schulz⁶ and by Jarmie, Repp, and White.⁷

The most extensive measurements to date in the region 200 to 300 Mev have been those performed at Cornell with a double focusing magnetic analyser, and targets of polyethylene and carbon.⁸ The Cornell group finds that the angular distribution at 200, 235, and 265 Mev is peaked in the backward hemisphere in agreement with the data of Steinberger and Bishop. The cross section increases with energy in this region.

The behavior of the photopion production near threshold is of considerable interest, and has been extensively investigated at Illinois using photographic plates to detect positive mesons produced in a liquid hydrogen target.⁹ Measurements at low energies have also been made at CalTech using photographic plates¹⁰ and at the Massachusetts Institute of Technology using counter techniques involving a $\pi-\mu-e$ decay detection scheme¹¹ and a $\pi-\mu$ detection scheme.¹²

When the present experiments were begun, in June, 1953, we were especially interested in finding the behavior of the angular distribution above 300 Mev. The suggestion¹³ that there might be a resonant interaction between pion and nucleon in a $P_{\frac{1}{2}}$ state of isotopic spin $\frac{3}{2}$ was consistent with pion-nucleon scattering data, and could perhaps explain the marked peak in the photoproduction of neutral pions at 90° , near 300 Mev.¹⁴

* This work was supported in part by the U. S. Atomic Energy Commission.

¹ See, for example: Anderson, Fermi, Martin, and Nagel, *Phys. Rev.* **91**, 155 (1953).

² For a review of the experimental data and analysis, and a list of references to the original work, see the forthcoming book: H. A. Bethe and F. de Hoffmann, *Mesons and Fields* (Row, Peterson, and Company, Evanston), Vol. 2.

³ de Hoffmann, Metropolis, Alei, and Bethe, *Phys. Rev.* **95**, 1586 (1954).

⁴ H. A. Bethe and F. de Hoffmann, *Phys. Rev.* **95**, 1100 (1954).

⁵ J. Steinberger and A. S. Bishop, *Phys. Rev.* **86**, 171 (1952).

⁶ White, Jacobson, and Schulz, *Phys. Rev.* **88**, 836 (1952).

⁷ Jarmie, Repp, and White, *Phys. Rev.* **91**, 1023 (1953).

⁸ Jenkins, Luckey, Palfrey, and Wilson, *Phys. Rev.* **95**, 179 (1954).

⁹ G. Bernardini and E. L. Goldwasser, *Phys. Rev.* **94**, 729 (1954); *Phys. Rev.* **95**, 857 (1954).

¹⁰ Vincent Peterson and I. George Henry, *Phys. Rev.* **96**, 850 (1954).

¹¹ Goldschmidt-Clermont, Osborn, and Winston, *Phys. Rev.* **91**, 468 (1953).

¹² G. S. Janes and W. L. Kraushaar, *Phys. Rev.* **93**, 900 (1954).

¹³ K. Brueckner, *Phys. Rev.* **86**, 106 (1952).

¹⁴ Walker, Oakley, and Tollestrup, *Phys. Rev.* **89**, 1301 (1953).

Calculations of photoproduction based on this idea had already been given by Brueckner and Watson.¹⁵ If such a resonant interaction exists, one might expect the forward-backward asymmetry in the photopion production, which must arise from an interference between even and odd states, presumably *S* and *P*, to change sign at energies above the resonance. We find that this does, in fact, occur, and that the total cross section falls off very rapidly at energies above 300 Mev as might be expected from the resonance idea.

METHOD

Since the photoproduction of a pion in hydrogen is a two-body process, a measurement of the energy and angle of the emitted meson determines uniquely the energy k of the photon producing the reaction

$$\gamma + p \rightarrow \pi^+ + n. \quad (1)$$

This fortunately makes it possible to measure the cross section at a specific photon energy in spite of the continuous bremsstrahlung spectrum from a synchrotron. The present experiment consists of counting the number of mesons produced at a given angle as a function of the meson energy, measured with a magnetic spectrometer. From the laws of conservation of energy and momentum, it is easy to find the following relation between the photon energy k and the pion momentum p_π , and angle θ_π .

$$k = \frac{m_p E_\pi - \frac{1}{2}(m_\pi^2 - m_n^2 + m_p^2)}{m_p - E_\pi + p_\pi \cos \theta_\pi}, \quad (2)$$

where m_π , m_p , and m_n are the masses of pion, proton, and neutron, respectively,¹⁶ and $E_\pi = (p_\pi^2 + m_\pi^2)^{1/2}$ is the total energy of the pion. The range of photon energies, Δk , corresponding to the range of momentum, Δp_π , accepted by the spectrometer, may be found by multiplying Δp_π by the factor,

$$\frac{\partial k}{\partial p_\pi} = \frac{p_\pi(m_p + k) - kE_\pi \cos \theta_\pi}{E_\pi(m_p - E_\pi + p_\pi \cos \theta_\pi)}. \quad (3)$$

The differential cross section $\sigma(\theta)$ is related to the observed counts C per standard beam monitor reading through the formula

$$C(k) = \sigma(\theta) \Delta \Omega N(k) \Delta k N_H R(k), \quad (4)$$

where $\Delta \Omega$ is the solid angle accepted by the spectrometer. $N(k) \Delta k$ is the number of photons of mean energy k within an energy interval Δk in the Bremsstrahlung beam. This number is known from an absolute beam calibration to be discussed later. N_H is the number of target hydrogen atoms per cm². $R(k)$ is a correction factor for the effect of decay of the pions before reaching the counters. It will be discussed in a later section. The

¹⁵ K. Brueckner and K. M. Watson, Phys. Rev. **86**, 923 (1952).

¹⁶ A positive pion mass of 139.6 Mev/c² was used in the calculations.

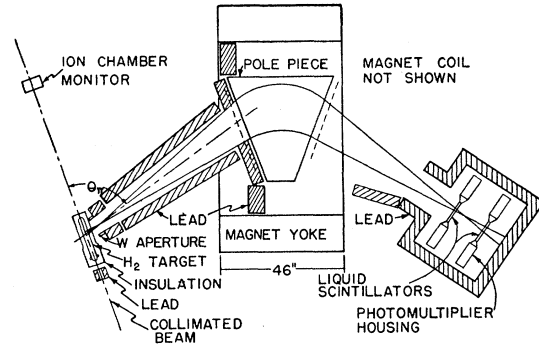


FIG. 1. Diagram of the magnetic spectrometer and the gas target.

preliminary reports of the present data¹⁷ made use of a rough calculation of the decay correction, and differ a little from the final results reported here.

The values of k and Δk obtained from the simple formulas (2) and (3) have been corrected for energy loss of the pions in the walls of the target, as will be discussed in the next section.

APPARATUS

The experimental arrangement is shown in Fig. 1. The photopions are produced in a high-pressure hydrogen gas target located about 8 meters from the internal synchrotron target. The beam is collimated to 3.8 cm in diameter at the target by a primary lead collimator which is backed up by successively larger holes in two other lead collimators, the final one located immediately in front of the target. The hydrogen gas is contained at about 2000 psi in a bomb 2 inches in diameter and 17 inches long with 0.030-inch steel walls. This is connected to a liquid nitrogen reservoir, and surrounded by about 1.5 inches of styrafoam insulation, so that the hydrogen can be cooled to about 95°K, resulting in a typical gas density of 0.030 g cm⁻³.

The density is obtained from a pressure measurement accurate to about one percent, and a temperature measurement of approximate accuracy three percent. The temperature is read at the two ends of the bomb with thermocouples, the reference junction being in the liquid nitrogen reservoir, at the temperature 77°K.

The thicknesses of the steel target walls, the styrafoam insulation, and the air path between target and magnet are not negligible in stopping power for the mesons. Thus a small correction must be made for energy loss of the pions before they enter the magnet. This correction shifts the photon energy k calculated from formula 2 by 4 to 12 Mev, depending on the meson angle and energy. This energy loss also influences the momentum range Δp_π accepted by the spectrometer, and thus the photon interval Δk . The resulting correction to the cross section amounts to only 1 to 3 percent in general, but becomes as high as 12 percent at lowest energies.

¹⁷ Walker, Teasdale, and Peterson, Phys. Rev. **92**, 1090(A) (1953).

The energy analysis of the pions emitted at a given angle is made with a conventional magnetic analyser having wedge-shaped pole pieces as shown in Fig. 1. Two geometrical arrangements were used, one capable of measuring higher energy mesons than the other. The "short-focus" arrangement (shown in Fig. 1) has a focal distance (from the edge of the pole piece to the focal point) of 170 cm and a radius of curvature of 72 cm. This is suitable for measuring mesons of energies up to 200 Mev, using the maximum magnetic field of 15 000 gauss. A second "long-focus" arrangement has a focal distance of 254 cm, a radius of curvature of 98 cm, and can be used for meson energies up to 300 Mev. Neither arrangement is double focusing although in both some "focusing" in the vertical direction occurs in the fringe field of the magnet.¹⁸

The fringe field has been measured as a function of distance from the pole tip edge, and its effect on the path of the particles is included in the relation between particle momentum and magnetic field. The field was calibrated as a function of magnet current by means of a proton resonance magnetometer.

The counters are high enough for the short-focus arrangement to cover the full vertical height of the "image" as limited by a three-inch vertical aperture at the magnet entrance. This is not quite true for the long-focus arrangement. Thus, a correction to the solid angles for the long-focus measurements was made for the pions missing the counters above or below. This correction of 6 ± 3 percent was determined experimentally by counting protons from the target with the normal 3-inch magnet aperture and with an aperture decreased to 2 inches, for which the counters are definitely high enough.

The momentum resolution of the spectrometer is determined mainly by the width of the counters which is 9 inches. This gives a momentum range Δp accepted of approximately $\Delta p = (0.090)p$ for both long- and short-focus arrangements. The solid angle of acceptance is determined by the lead aperture at the magnet entrance. It varied from 0.002 to 0.011 steradian in the present experiments. The effective length of target seen by the spectrometer is defined by tungsten lined slits placed at the focal point of the magnet and as near to the target as possible. These slits, and the edges of the magnet aperture were tapered to minimize the uncertainties arising from slit penetration.

Mesons are counted by two large scintillation counters in coincidence. Each is a liquid scintillation cell of dimensions $6 \times 9 \times 1$ inches, viewed by two RCA 5819 photomultipliers connected to the two ends of the cell by short Lucite light pipes. These counters are enclosed in lead shielding 4 inches thick on all sides, and additional lead shielding is placed along the sides of almost the entire meson path as shown in Fig. 1.

It was appreciated too late, unfortunately, that some

¹⁸ See for example E. Segrè, *Experimental Nuclear Physics* (John Wiley and Sons, Inc., New York, 1953), Chapter by K. T. Bainbridge, pp. 576 ff.

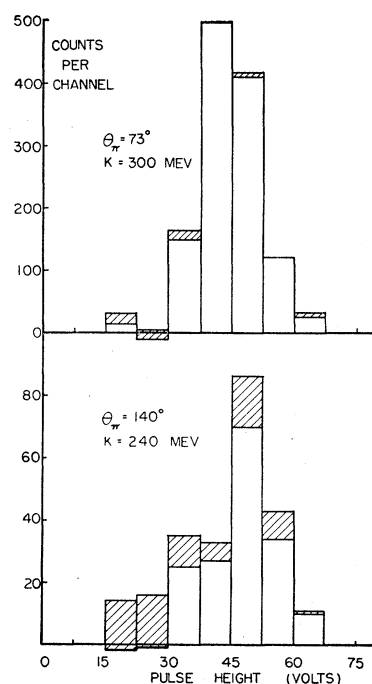


FIG. 2. Pulse-height spectra from the front counter, showing the pion peak. Background, as measured with the magnetic field of the spectrometer reversed, is shown by the cross-hatched areas. The two spectra are chosen from among the best and the worst obtained during the experiment.

mesons which scatter from this shielding pass through the counters, so a 10 percent correction must be made for this scattering. The experimental information for this correction is given in item C3 under "Errors."

Pulses from the two counters are amplified with amplifiers having rise times of about $0.07 \mu\text{sec}$ and delay line clippers giving pulses about $0.5 \mu\text{sec}$ long. These trigger pulse shaping circuits which form the inputs to a coincidence circuit with resolving time of $0.1 \mu\text{sec}$. The coincidence circuit output is used to gate an 8-channel pulse-height analyzer which measures the pulse-height in the front counter. This is helpful in separating counts caused by mesons from background counts. Sample pulse-height spectra are shown in Fig. 2, the two curves having been chosen from the best and worst obtained during the experiment. This pulse-height analysis can be used at low energies to help distinguish mesons from electrons. Chance coincidence counts are monitored by a duplicate coincidence circuit having a $1\text{-}\mu\text{sec}$ delay in one input. The chance coincidences were 1 to 6 percent of the true counts in general, but in some cases became as high as 15 percent.

IDENTIFICATION OF PIONS

The magnet directs all particles having the appropriate momentum into the counters, and it is necessary to count from these only the number of pions, or in practice, pions plus decay muons. Discrimination against protons is very simple since protons of the same momenta

as the pions observed in these experiments have very much smaller ranges than the pions. Thus a small thickness of lead absorber between the two counters prevents any coincidences from protons. Discrimination against positrons is more difficult, except at the lowest energies, where the ionization of pions in the first counter is appreciably above minimum, so that the pion pulse height peak is shifted above that of electrons. However, since one may expect the numbers of high-energy electrons and positrons to be about equal, it is easy to subtract the positron background by making a measurement with the magnetic field reversed. Fortunately, these negative field backgrounds were not high for most of the measurements, although they become large at the extreme angles. The magnitude of these backgrounds is given in Table I. At 12.5° no slits could be used at the target so the ends of the bomb were in view of the magnet, and the electron background was quite serious. The electron counts could be reduced to 25 to 50 percent for the high-energy points by using 5 cm of lead absorber between the two counters. For the lower energies where the mesons could not safely penetrate this thickness of absorber, no measurements could be made.

Incidentally, the procedure of subtracting electron backgrounds taken with the magnetic field reversed also eliminates counts which might arise from the possible production of positive and negative pion pairs. This experiment measures the cross section for single pion production.

The number of high-energy electrons emitted from the hydrogen target at angles of 30° or more is small, of course, because the usual shower processes of pair production, bremsstrahlung, Compton scattering, and electron scattering, occur at very small angles in hydrogen. In fact, it seems likely that most of the electrons which we do observe at the central angles originate from π^0 decay photons converted in the target wall or elsewhere.

As a test of the fact that the counts observed are actually caused by mesons, we measured the absorption curve in lead for the particles being counted (with the electron background subtracted). One such range curve is reproduced in Fig. 3. This shows that most of the particles have the range corresponding to pions, al-

TABLE I. Negative field backgrounds.

Lab angle	Negative field counting rate/ π^+ counting rate		
	Low-energy region	Central energies	High energies
12.5° L.F. ^a	1.0-2.0	0.5-0.8	0.23-0.4
30° S.F.	0.4-0.6	0.07-0.4	0.04-0.07
30° L.F.	0.30-2.0	0.13-0.30	0.18-0.27
51° S.F.	0.10-0.26	0.04-0.10	0.04-0.06
51° L.F.	0.06-0.13	0.04-0.10	0.07-0.10
73° S.F.	0.09-0.17	0.04-0.06	0.04-0.05
104° S.F.	0.03-0.06	0.02-0.04	0.03-0.10
140° S.F.	0.15-0.46	0.10-0.30	0.30-0.36
180° S.F.	1.0-1.6	1.3	2.7-3.4

^a L.F. and S.F. indicate long- and short-focus arrangements, respectively.

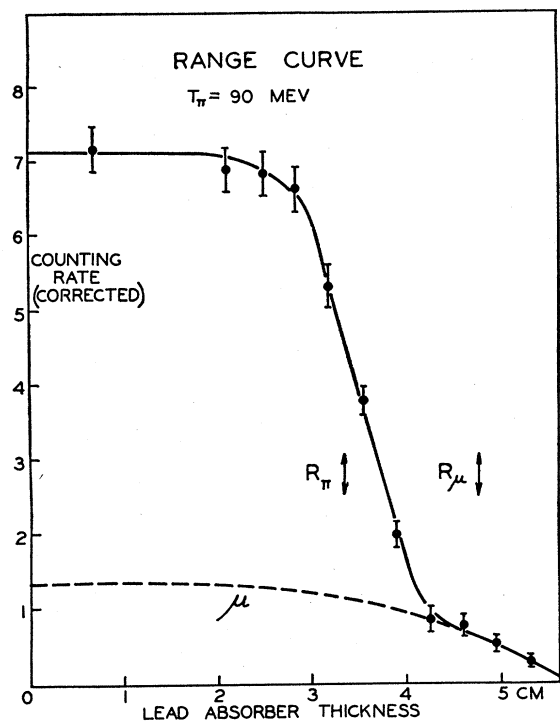


Fig. 3. Range curve for the particles observed at 73° with momentum corresponding to 90-Mev pions. The tail is probably due to muons from $\pi-\mu$ decay in flight. The curve marked μ indicates the fraction of counts expected to come from muons according to the calculations made for the decay correction. The pion counting rate has been corrected for nuclear absorption in the lead absorber.

though a tail of longer-range particles is present. This tail is expected since we have no good way to separate decay muons from the pions. Corrections for $\pi-\mu$ decay involve a calculation of the number of muons counted compared to the number of pions. The height of the dashed curve marked μ in Fig. 3 is taken from these decay correction calculations, which are described in a later section.

The range curve of Fig. 3 has been corrected for nuclear absorption of the pions in the lead absorber. In fact, all the data taken for the cross-section measurements have been corrected for nuclear absorption in the target walls, in the front counter, and in the lead absorber (if any) between the two counters. The absorption cross sections assumed were "geometrical," corresponding to a mean free path of 160 g cm^{-2} of lead, for example. This nuclear absorption correction factor amounts to 0.95 to 0.90 in most of the present measurements, but is 0.62 for the 12.5° data.

INCIDENT PHOTON SPECTRUM

To obtain the absolute differential cross section from the number of counts observed, one must know the number of photons in the collimated beam per unit energy range at energy k . This number, the $N(k)$ of Eq. (4), is normalized to a standard beam monitor reading, as are the observed counts, C . The beam

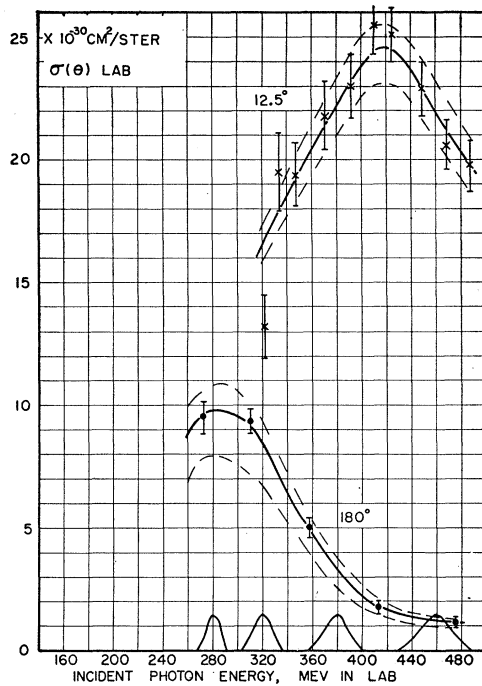


FIG. 4. Excitation curves at laboratory angles 12.5° and 180° , taken with the long-focus arrangement (crosses) and short-focus arrangement (circles), respectively. The differential cross section in the laboratory system is plotted as a function of photon energy. The resolution functions shown at the bottom are approximately correct for both sets of data.

monitor is an air ionization chamber similar to the one designed at Cornell, with one-inch-thick copper walls in which a shower is generated, the shower maximum falling approximately at the ion collection region. The ionization charge produced by the beam is integrated by a circuit which is similar to those described by Lewis and Collinge¹⁹ and by Littauer.²⁰ The charge collected from this chamber is very nearly proportional to the total energy in the synchrotron beam, independent of the synchrotron energy. (The constant of proportionality is 10 or 12 percent less at 500 Mev than at 300.) In addition to this feature, the thick walls of the chamber make it insensitive to its nearby surroundings. For example, the reading is very little affected by stacks of lead behind or at the sides of the chamber.

The calibration of the synchrotron beam, i.e., the measurement of the total energy in the beam corresponding to a given charge collected from this ion chamber, has been made by two methods in this laboratory. One involves a measure of the total energy liberated in a shower produced in aluminum, by a method similar to that of Blocker, Kenney, and Panofsky.²¹ This was done by J. C. Keck. The other consisted of measuring the photon spectrum $N(k)$ with a

¹⁹ I. A. D. Lewis and B. Collinge, *Rev. Sci. Instr.* **24**, 1113 (1953).

²⁰ Raphael Littauer, *Rev. Sci. Instr.* **25**, 148 (1954).

²¹ Blocker, Kenney, and Panofsky, *Phys. Rev.* **79**, 419 (1950).

pair spectrometer whose absolute efficiency is known. These measurements will be described elsewhere.²² The shape of the photon spectrum observed with the pair spectrometer agrees with the theoretical Bremsstrahlung shape within the experimental accuracy of three or four percent. Each of the two beam calibration methods has an estimated accuracy of about 5 percent, but the results disagree unfortunately by 15 percent. The pair spectrometer calibration gives $Q = 4.75 \times 10^{18}$ Mev/coulomb. The shower method gives $Q = 4.12 \times 10^{18}$. Thus until further work is done to clear up this discrepancy, we use $Q = 4.44 \times 10^{18}$ Mev per coulomb at STP for these experiments.²³

The photon spectrum $N(k)$ near the upper end, i.e., near the synchrotron energy, E_0 , depends on how the electron beam of the synchrotron is "spilled out." In these counter experiments, the beam was spread out for about 15 milliseconds at the peak of the magnetic field, giving a duty cycle of 0.015. This results in a spread of electron energies of about 15 Mev, and a resulting region of uncertainty at the upper end of the spectrum. From the pair spectrometer measurements, taken under these same conditions, we conclude that measurements at energies 450 Mev or below, with resolution similar to that of the present experiments, are not influenced by

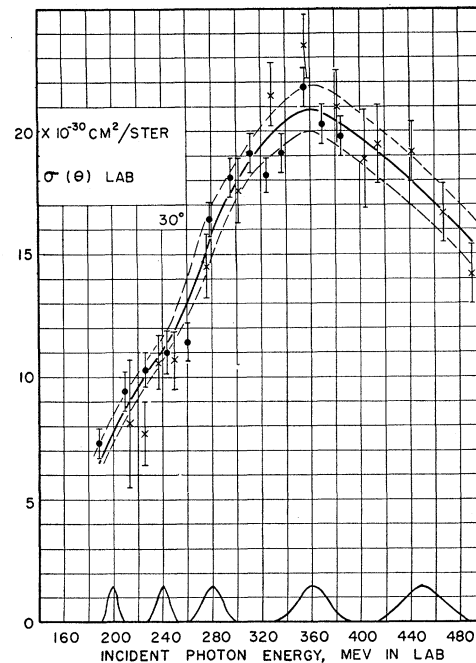


FIG. 5. Excitation curve at laboratory angle 30° . The points shown by crosses in this data and in the 51° data of Fig. 6 were obtained with the long-focus arrangement. The points indicated by circles in all the excitation curves were obtained with the short-focus arrangement.

²² D. H. Cooper, thesis, California Institute of Technology, 1954 (unpublished).

²³ This corresponds to 3.91×10^{18} Mev/coulomb at 300 Mev, compared to the Cornell calibration of 3.71×10^{18} . For this reason alone, our cross sections would be 5 percent lower than those measured at Cornell (and Illinois).

the uncertainties of the upper end of the bremsstrahlung spectrum. The synchrotron energy E_0 as measured with the pair spectrometer is 500 to 505 Mev.

180° DATA

Some relatively uncertain measurements were made at a meson angle of 180°, and since the conditions applying to these measurements are somewhat special, they are described in this section. Obviously the photon beam must pass through the spectrometer magnet before hitting the target so that background troubles are apt to become serious.

This background was reduced as much as possible by appropriate lead shielding, and by evacuating the magnetic field region of the spectrometer. The beam entered and left this region through long evacuated tubes capped with thin aluminum windows. Even with these precautions, the backgrounds were as high or higher than the meson counting rates. Furthermore, if mesons were to come through the cylindrical target wall at a very small angle, the effective wall thickness would be quite large. Thus, the magnet entrance aperture was reduced to 8.4 cm in diameter so that only mesons coming through the hemispherical end cap of the target would be accepted. Nevertheless, this geometry makes the measurement rather sensitive to scattering effects in the bomb walls. Fragmentary calculations of a portion of these scattering effects have been made and gave no corrections for this portion. However, it seems likely that the scattering effects would increase the flux of pions out of the ends of

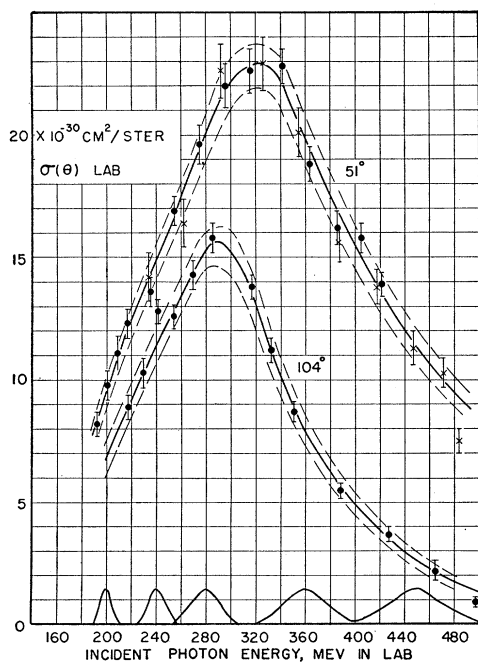


FIG. 6. Excitation curves at laboratory angles 51° and 104°. The resolution curves are for the 51° data. Those for the 104° data are approximately 15 percent wider at low energy and 50 percent wider at high energy.

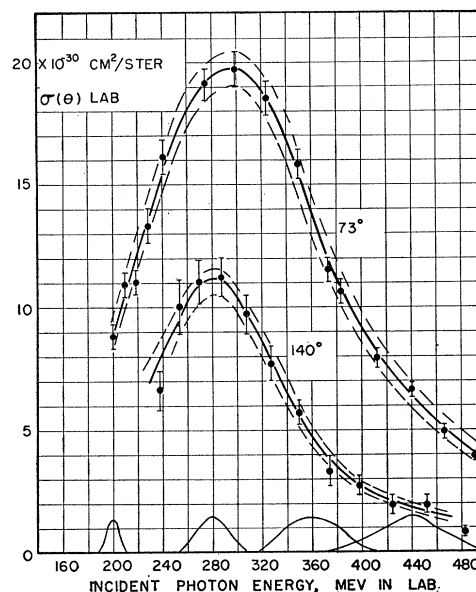


FIG. 7. Excitation curves at laboratory angles 73° and 140°. The resolution curves are for the 73° data. Those for the 140° data are approximately 25 percent narrower.

the target, and thus give cross sections that are too high since no corrections have been made. A somewhat arbitrary error of +10, -20 percent has been assigned for this effect. Thus, the 180° cross sections are probably good as upper limits, but they have not been included in the least squares fits of the angular distributions. Good measurements at 180° could probably be made using a liquid hydrogen target.

RESULTS

The differential cross section as a function of energy at each of the laboratory angles measured, is shown in Figs. 4, 5, 6, and 7. These cross sections are calculated, using relation 4, from the observed counting rates after making the various corrections already mentioned.

The data of Figs. 4 to 7 have been analyzed to obtain angular distributions in the center of momentum system at energies from 200 to 470 Mev, in 30 Mev intervals. These angular distributions are shown in Figs. 8, 9, and 10. The points shown are simply the cross sections taken from the solid curves of Figs. 4 to 7, converted to the center of momentum system and plotted at the center of momentum angle. The errors include both random statistical errors and systematic errors which affect the shape of the angular distributions.

The solid curves of Figs. 8, 9, and 10 are derived from a least-squares fit of the data to the form

$$\sigma(\theta) = A + B \cos\theta + C \cos^2\theta. \quad (5)$$

The values of the coefficients A , B , and C thus obtained are given in Fig. 11. The most striking feature of the angular distributions is the shift from a backward maximum at low energies to a forward maximum at high

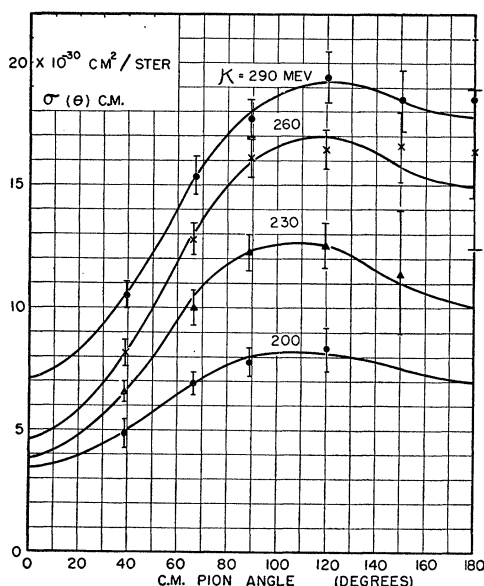


FIG. 8. Angular distributions. The differential cross section in the center of momentum system is given as a function of the c.m. pion angle for incident photon energies 200, 230, 260, and 290 Mev in the laboratory. The errors on the points represent both the random statistical errors, and those systematic errors which affect the shape of the angular distribution. The solid curves are obtained from least squares fits of the angular distributions to the form $\sigma(\theta) = A + B \cos\theta + C \cos^2\theta$.

energies. This is described, of course, by the coefficient B changing sign near 340 Mev.

The total cross section,

$$\sigma = 4\pi(A + C/3), \quad (6)$$

is given in Table II. The total cross section divided by the square of the incident photon wavelength λ in the

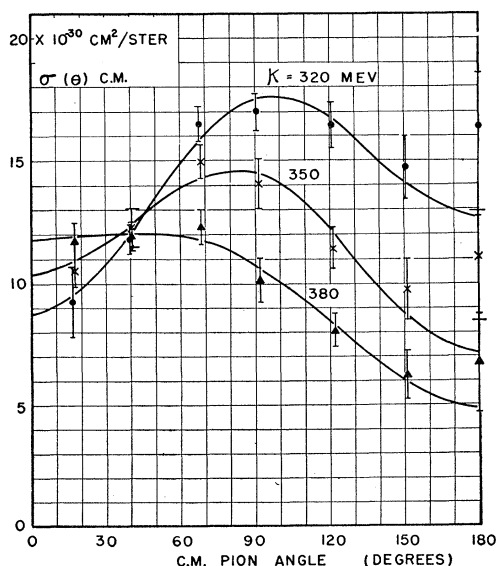


FIG. 9. Angular distributions at incident photon energies 320, 350, and 380 Mev.

c.m. system is shown as a function of the photon energy in Fig. 12.

DECAY CORRECTIONS

The distance between the target and counters in the magnetic spectrometer is long, so that the pions have an appreciable probability of decaying before reaching the counters. If one assumes the mean life for $\pi-\mu$ decay $\tau = (2.55 \pm 0.11) \times 10^{-8}$ sec,²⁴⁻²⁶ it is a simple matter to calculate the fraction of pions which arrive at the counters before decay. This is plotted as the curves marked R_π in Figs. 13 and 14. If a pion decays before reaching the counters, the decay muon may still pass through the two counters and be recorded. Furthermore, the counters will be traversed by some muons from the decay of pions which themselves would not have been counted, either because they have the wrong energy or direction of emission from the target. Since our counters cannot in general tell the difference between pions and

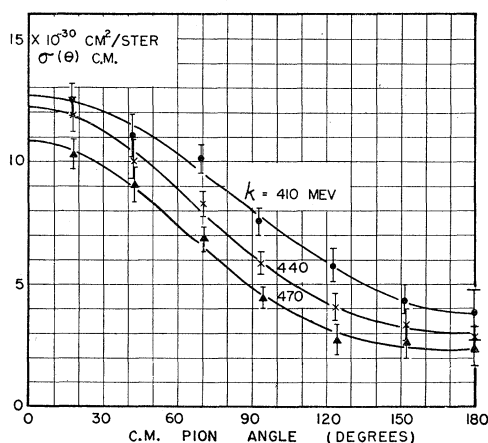


FIG. 10. Angular distributions at incident photon energies 410, 440, and 470 Mev.

muons, it is necessary to add to R_π the fraction R_μ of counts which come from decay muons, in order to obtain the decay correction factor, $R(k)$, of Eq. (4). A considerable effort has been spent calculating this correction factor, and we believe that it is accurate in general to about 5 to 7 percent. Since a description of the details of the method used for these calculations would be rather lengthy, and not of general interest,²⁷ only the results will be given, namely, Figs. 13 and 14. The calculations involve a computation of the number of muons which get into the counters from decays at various distances along the particle trajectory through the spectrometer. This takes into account the spectrum of pions at the angle of the spectrometer, (this spectrum is obtained from the measurements, using a preliminary

²⁴ Jacobson, Schulz, and Steinberger, Phys. Rev. **81**, 894 (1951).

²⁵ C. E. Wiegand, Phys. Rev. **83**, 1085 (1951).

²⁶ Durbin, Loar, and Havens, Phys. Rev. **83**, 179 (1952).

²⁷ A description of the procedure used in these calculations is available for those interested.

value for the decay corrections); the $\pi-\mu$ decay dynamics, both in energy and angle; geometrical properties of the spectrometer; and the fact that the muons will not count if their range is too small to get into the second counter. Fortunately, the decay position making the greatest contribution to the muon counting rate is at the source, where the calculation is both simple and accurate, involving simply a conversion of the observed pion spectrum to a spectrum of decay muons.

ERRORS

The errors have been classified into three types: (All errors quoted are intended to be standard statistical errors).

(A) *Errors in the absolute cross section* which are independent of meson energy and angle.

- (1) Beam calibration: 7 percent.
- (2) Average H_2 gas density: 3 percent.
- (3) Part of the $\pi-\mu$ decay correction, R : 4 percent.
- (4) Part of the correction for scattering from the lead shielding: 4 percent.
- (5) Error in the momentum range, Δp , accepted by the spectrometer: 2 percent.

TABLE II. Total cross sections in units 10^{-30} cm². The errors are obtained from the least-squares fits of the angular distributions. Errors of type *A* are not included.

k (Mev)=200	230	260	290	320
$\sigma(\mu b)=89\pm 7$	133 \pm 6	175 \pm 5	204 \pm 5	192 \pm 5
k (Mev)=350	380	410	440	470
$\sigma(\mu b)=158\pm 5$	125 \pm 4	102 \pm 3	84 \pm 3	68 \pm 3

The resulting over-all error in absolute values of the cross sections is about 10 percent.

(B) *Random statistical errors* which fluctuate from point to point. These are indicated as errors on the individual points in the excitation curves of Figs. 4, 5, 6, and 7. They are mainly counting errors arising from the limited numbers of counts, and from uncertainty in the determination of upper and lower limits for the meson peaks such as shown in Fig. 2. However, included in these random errors are the effects of those variations in the temperature of the ion chamber monitor, the target gas density, and the synchrotron energy, which could not be corrected.

(C) *Systematic errors which vary smoothly* from point to point on an excitation curve or angular distribution. These are indicated on the excitation curves by dashed curves on either side of the solid one. These errors include the following:

- (1) Part of the $\pi-\mu$ decay correction error: 2 to 6 percent (typically 4 percent).
- (2) Error in the nuclear absorption cross section: 10 percent of the absorption cross section. This amounts to an error in the correction factor of 1 to 2 percent except for the 12.5° data where it is 5 percent.

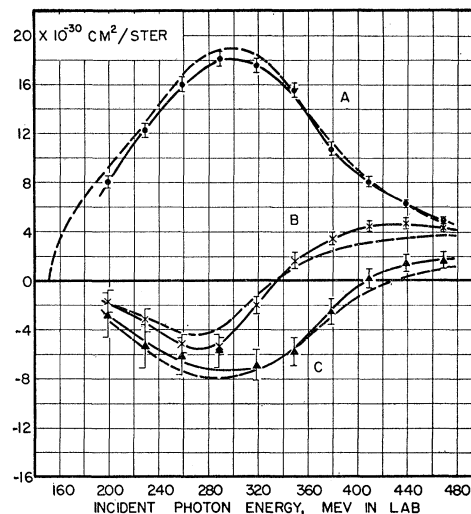


FIG. 11. Coefficients A , B , and C obtained by a least-squares fit of the angular distribution to the form $\sigma(\theta) = A + B \cos\theta + C \cos^2\theta$. The dashed curves give the "average" experimental coefficients of Table III, taking into account all the data shown in Fig. 15.

(3) Error in the correction for scattering from the lead shielding: 3 percent. This correction was measured experimentally at $\theta_\pi = 49^\circ$ by taking data with the lead shielding very far apart and comparing to the counts obtained with the shielding normal. This gave the following results for this scattering correction:

$$\begin{aligned}
 k = 200 \text{ Mev: } & 1.092 \pm 0.070, \\
 k = 300 \text{ Mev: } & 1.089 \pm 0.029, \\
 k = 400 \text{ Mev: } & 1.126 \pm 0.024.
 \end{aligned}$$

This shows no definite or sensible variation with energy, so a uniform correction of 10 percent has been applied to all the data.

- (4) Slit penetration errors: 1 to 2 percent.
- (5) Uncertainties in the angle $\theta_\pi (\pm 1^\circ)$ and in meson

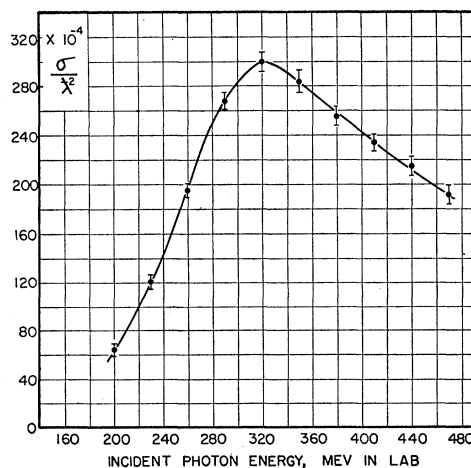


FIG. 12. The total cross section σ divided by λ^2 . $2\pi\lambda$ is the c.m. photon wavelength.

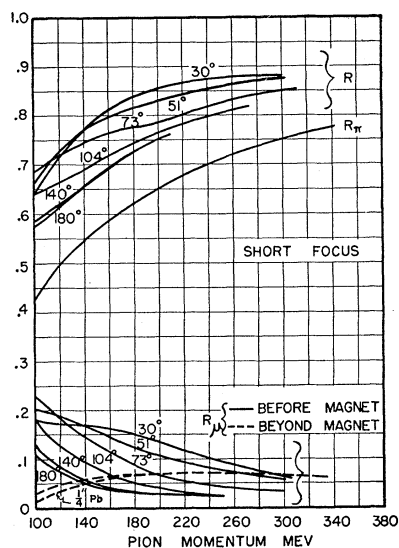


FIG. 13. Decay corrections for data obtained with the short-focus arrangement. See section on decay corrections.

momentum (± 1 percent) as they affect the cross section: 1 to 3 percent.

(6) Uncertainty in solid angle because the counters are not sufficiently high: 3 percent for long-focus measurements only.

COMPARISON WITH OTHER EXPERIMENTS

An experiment described in an accompanying paper has been done in this laboratory²⁸ by using a counter telescope to measure these same cross sections. These two experiments are completely independent except for

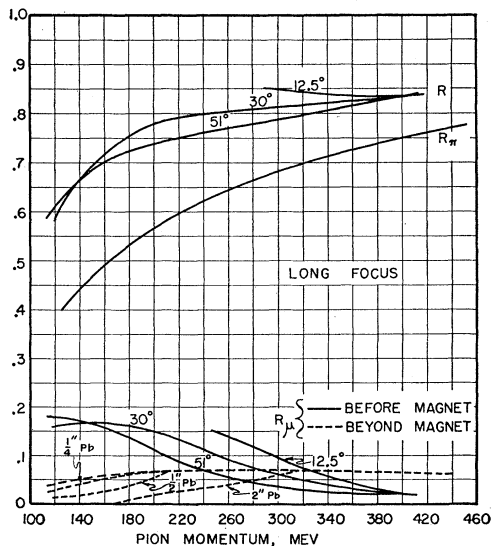


FIG. 14. Decay corrections for data obtained with the long-focus arrangement.

²⁸ Tollestrup, Keck, and Worlock, following paper [Phys. Rev. 99, 220 (1955)].

the beam monitor and the hydrogen target gas density. (The two sets of data were taken simultaneously, using the same target.) Furthermore, the two experiments have different difficulties in general. For example, the effects of $\pi-\mu$ decay are large for the magnet experiment, especially at low energies, but are quite unimportant for the telescope experiment. On the other hand, corrections for nuclear absorption in the stopping material become large for the telescope data, especially at high energies, but are not very important for the magnet data.

The data obtained by the two methods agree well in their general features, but differ some in detail. At low energies, the magnet data are low compared to the telescope data in the forward direction, and high in the

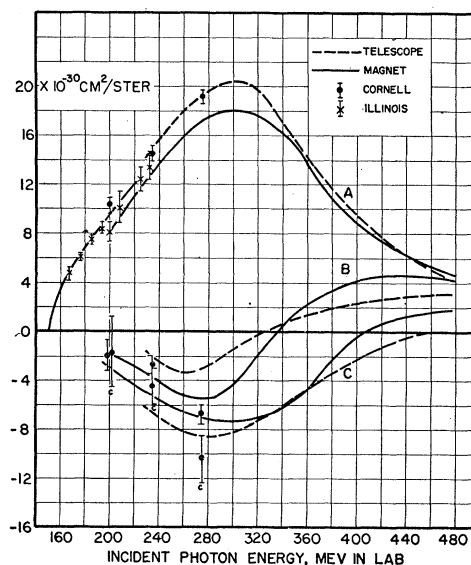


FIG. 15. Comparison with other experiments. The solid curves are reproduced from Fig. 11 for the present experiment. The dashed curves are the corresponding ones from the telescope data of Tollestrup, Keck, and Worlock. The Cornell data of Jenkins, Luckey, Palfrey, and Wilson (see reference 8) are shown by the circle points; and the Illinois data of Bernardini and Goldwasser (see reference 9) are shown by the crosses and solid curve for A at low energies.

backward direction. At high energies, the magnet data are considerably higher in the forward direction. These differences result in a smaller coefficient B of the $\cos\theta$ term in the angular distribution for the telescope data than for the magnet data. This may be seen in Fig. 15, where the curves of Fig. 11 giving the coefficients A , B , and C are reproduced together with the corresponding curves from the telescope experiment.

The data of Jenkins, Luckey, Palfrey, and Wilson⁸ at Cornell are also compared to the present data in Fig. 15 by giving the coefficients A , B , and C from the Cornell experiment. The agreement with the present data is reasonably good.

The low-energy 90° measurements of Bernardini and Goldwasser⁹ are also shown in Fig. 15. These were ob-

tained with the Illinois betatron by using photographic plate detection and a liquid hydrogen target. These data fit rather well onto the coefficient A of the present experiment.

For use in comparison with theory, we have tried to draw an average experimental curve for all the data shown in Fig. 15, for each of the three coefficients. The curve for A follows the values of Bernardini and Goldwasser at low energy, then the average of the CalTech magnet and telescope data at high energy. The curves for B and C are essentially the average of the magnet and telescope data. All three curves are given an energy dependence at threshold expected theoretically, i.e., approximately $(k-k_0)^{1/2}$, $(k-k_0)$, and $(k-k_0)^3$ for A , B , and C , respectively. k_0 is the threshold photon energy 151 Mev. These curves are shown in Fig. 11 by dashed curves, and values of the average A , B , and C are given in Table III at 30-Mev intervals.

INTERPRETATION

Several more or less phenomenological descriptions of pion photoproduction have been given.^{15,29-33} Most of these relate the photoproduction to pion nucleon scattering since the pion-nucleon interaction plays a dominant role. Chew³¹ has used a cutoff form of meson theory to calculate the photoproduction as well as the scattering. The most satisfactory theory at present for comparison with experiment is the phenomenological one of Gell-Mann and Watson,³³ as extended recently by Watson.³⁴ This (and also the other theories) gives a description in terms of photoproduction into states of definite angular momentum and isotopic spin. Thus a full comparison with experiment must treat the production of charged and neutral pions together. Such an analysis is being prepared in collaboration with K. M. Watson, so not much analysis of the positive pion cross sections will be given here. However, it seems clear that the most striking features of the data may be explained by the idea of a resonance^{13,15} in the pion nucleon interaction in the state of angular momentum and isotopic spin $\frac{3}{2}$.

²⁹ B. T. Feld, Phys. Rev. **89**, 330 (1953).

³⁰ M. Ross, Phys. Rev. **94**, 454 (1954).

³¹ Geoffrey F. Chew, Phys. Rev. **95**, 1669 (1954).

³² K. M. Watson, Phys. Rev. **95**, 228 (1954).

³³ M. Gell-Mann and K. M. Watson, Ann. Rev. Nuc. Sci. **4**, 219 (1954).

³⁴ K. M. Watson, Lectures at California Institute of Technology during the summer, 1954 (unpublished).

TABLE III. Average experimental values of the coefficients A , B , and C in the center-of-momentum angular distribution: $\sigma(\theta) = A + B \cos\theta + C \cos^2\theta$. These averages include all the data shown in Fig. 15, from CalTech, Cornell, and Illinois. The errors are estimates based on the accuracy of individual experiments and on the degree of consistency among different experiments. Since these values of A , B , and C have been taken from smooth curves, the values at neighboring energies are correlated, and the errors indicate merely the estimated accuracy of the coefficients in this energy region.

k (Mev)	A	B (units 10^{-30} cm ² /sterad)	C
170 Mev	5.2±0.5		
200	9.3±0.5	-1.8±1.0	-3.3±1.6
230	13.1±0.5	-3.0±0.9	-5.7±1.0
260	16.9±0.5	-4.3±1.0	-7.4±1.0
290	18.9±0.5	-3.8±1.2	-7.9±0.9
320	18.4±0.5	-1.1±0.9	-7.2±0.9
350	15.3±0.5	+1.1±0.6	-5.4±0.9
380	11.3±0.4	+2.5±0.6	-3.0±0.7
410	8.2±0.4	+3.2±0.8	-0.8±0.8
440	6.2±0.3	+3.5±0.7	+0.4±0.8
470	4.7±0.3	+3.7±0.6	+1.0±0.8

One of these features is, of course, the rapid decrease in the cross section above 320 Mev, appreciably faster than λ^2 . The other is the change in the angular distribution from a backward maximum at low energies to a forward maximum at high energies. In a simple "resonance" theory³³ the coefficient B of the $\cos\theta$ term contains a factor $[\cos(\alpha_{33}-\alpha_3) + 2 \cos(\alpha_{33}-\alpha_1)]$, where α_{33} , α_3 , and α_1 are the phase shifts for pion nucleon scattering in the $T=J=\frac{3}{2}$ p -state, and the two s -states of isotopic spin $T=\frac{3}{2}$ and $T=\frac{1}{2}$, respectively. According to the choice of phase shifts made by Bethe and de Hoffmann,⁴ in which a resonance is indicated by α_{33} going through 90°, the above factor changes sign at about 340 Mev. This agrees very well with the energy at which our coefficient B goes through zero.

ACKNOWLEDGMENTS

We are indebted to all the members of the synchrotron laboratory for contributions to this experiment, especially to Dr. R. F. Bacher for continual interest in the experiment and discussion of the results. Dr. M. L. Sands, D. C. Oakley, D. H. Cooper, and Paul Donoho helped take some of the data. These and Dr. R. V. Langmuir, Dr. A. V. Tollestrup, Dr. J. C. Keck, and our chief engineer, Bruce Rule, helped in the operation of the synchrotron.